LITERATURE CITED

1. Williams, J. A., L. Lowes and M. C. Tanner, *Trans. Inst. Chem. Engrs.*, **36**, 464 (1958).
2. Jeffreys, G. V., and J. L. Hawksley, *J. Appl. Chem.*, **12**, 329 (1962).
3. Kintner, R. C., *Can. J. Chem. Eng.*, **39**, 235 (1961).
4. Shinnar, R., and J. M. Church, *Ind. Eng. Chem.*, **52**, 253 (1960).
5. Rodgers, W. A., V. G. Trice and J. H. Rushton, *Chem. Eng. Progr.*, **52**, 12 (1966).

Part II. The Analysis of Coalescence in a Continuous Mixer Settler System by a Differential Model

Part II of this paper deals with the analysis of continuous separation of an unstable emulsion in a gravity settler of a mixer settler unit. When the emulsion passes from the mixing vessel into the settler, droplets of the dispersed phase approach one another to form a heterogeneous zone between the two liquid phases. The formation of this zone is determined by the local velocity gradients and the density difference between the phases. In the mixing zone, a high level of turbulence is generated to optimize mass transfer between two liquid phases, but in the settler all turbulence must be rapidly damped out, and the velocities of the phases in the settling tank must be low and controlled only by the throughput rates. The position of the heterogeneous layer with respect to the final interface between the settled phases will be determined by the density of the dispersed phase, and the liquid droplets in this layer tend to attain some stable packing arrangement determined by the diameter of the drops. It is important in any settling tank to prevent extract phase from being entrained with raffinate leaving the settler and vice versa. This difficulty can be overcome by suitable design and positioning of off-take lines and by operating the unit in such a way that the heterogeneous layer does not occupy the total available cross-sectional area between the phases in the settler. Under such conditions, the size of the heterogeneous wedge formed is determined by the throughput rates and by the physical properties affecting coalescence of the droplets, such as interfacial tension and viscosity of the liquids.

MODEL

Consider the behavior of the wedge of drops in more detail. Let the dispersed phase consist of drops of the more dense liquid; then the wedge is formed above the interface. At the lower surface of the wedge, droplets are coalescing with the bulk liquid phase by a drop-interface coalescence mechanism. Inside the wedge and at the upper surface, drops are coalescing together by a drop-drop coalescence mechanism. The residence time or life of the droplets in the wedge is controlled by these two processes.

Consider a settler of unit width operating under steady state conditions with the dispersed phase made up of the more dense liquid when a wedge of droplets will be formed above the interface, as shown in Figure 1. Consider a small increment δl in the wedge at a distance l from the inlet. Let the depth of the wedge at this position be h, let the number of drops entering the element per second be n, and let the mean diameter of the drops be ϕ. In practice, a distribution of drop sizes will exist at any position in the wedge. If uniform sized droplets enter the wedge, variation in sizes is brought about by variations in coalescence times. This will be discussed later in more detail. However, in this analysis a mean drop diameter will be considered. The volume of dispersed phase entering per second is equal to the volume of dispersed phase leaving the element, plus the volume of dispersed phase coalesced with the lower interface per second. Coalescence between droplets in the element will not affect the material balance. This mechanism of coalescence will result in an increase of the mean drop diameter in the element from ϕ to $\left(\phi + \frac{d\phi}{dl}\right)$. Thus, the material balance for the dispersed phase gives

$$\frac{n\pi\phi^3}{6} = \left(n - \frac{dn}{dl}\delta l\right)\frac{\pi}{6}\left(\phi + \frac{d\phi}{dl}\delta l\right)^3 + \frac{\pi\phi^3}{6}\left(\frac{1}{\tau^*}\frac{\delta l \eta^*}{\pi\phi^{2/4}}\right) \qquad (1)$$

The droplets have been considered as rigid spheres, and in the range of drop sizes studied in this work, 0.08 to 0.30 cm., this assumption is valid. Expanding Equation (1) and considering first-order terms only, we get

$$\frac{3}{\phi}\frac{d\phi}{dl} - \frac{1}{n}\frac{dn}{dl} + \frac{4}{\pi}\frac{\eta^*}{\tau^*}\frac{1}{n\phi^2} = 0 \qquad (2)$$

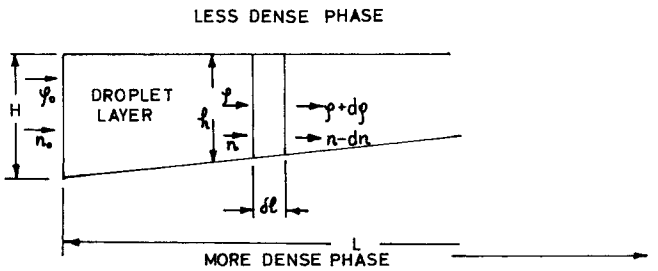

Fig. 1. Parameters of the differential model.

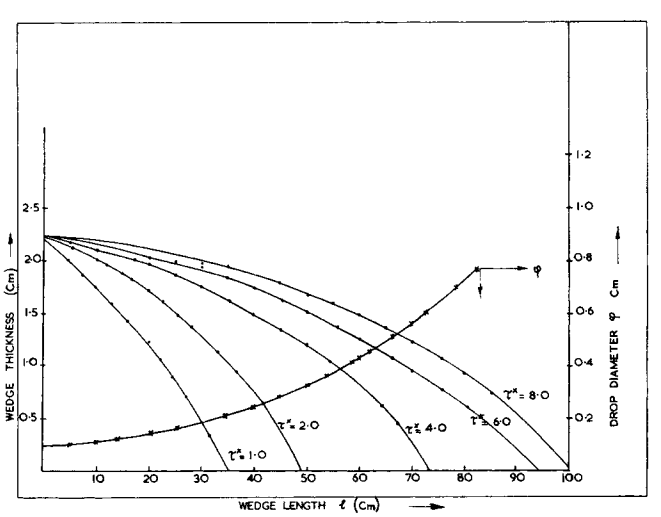

Fig. 2. Wedge thickness and drop diameter vs. wedge length. τ = 4.0 sec.

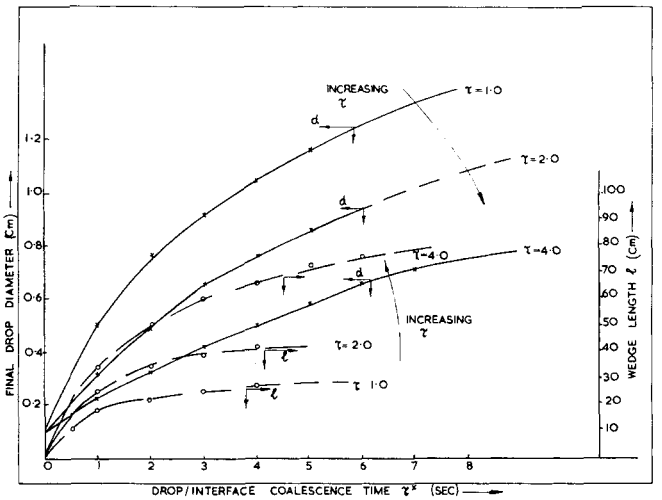

Fig. 3. Variation of the final drop diameter and wedge length with drop/interface coalescence time τ^* and drop-drop coalescence time τ.

In order to integrate this equation between the boundary conditions at the inlet ($\phi = \phi_0$, $n = n_0$) and at the end of the wedge, an equation relating the change in the average number of drops as a function of position within the wedge is required. Thus, assume that an average drop diameter at any position may be used to characterize that position in the wedge, then an equation can be derived to account for the change in the number of drops in any increment in the wedge. That is the number of drops entering the element per second must be balanced by the number of drops leaving, plus the number of drops coalescing at the interface and half the number of drops coalescing together by a drop/drop coalescence mechanism. Theoretically one should take into account coalescence steps between three and more drops, but as reference to such a behavior has not been reported in the literature, and the authors have not observed such effects in the experimental work carried out in these laboratories, multiple drop coalescence will be ignored. Thus, a drop balance gives

$$n = \left(n - \frac{dn}{dl}\delta l\right) + \left(\frac{\delta l}{\pi\phi^{2/4}} \cdot \frac{\eta^*}{\tau^*}\right) + \frac{1}{2}\frac{h\delta l\eta}{\left(\frac{\pi\phi^3}{6}\right)_\tau} \quad (3)$$

Rearranging Equation (3), we get

$$\frac{dn}{dl}\frac{1}{\phi^2}\left(\frac{3}{\pi}\frac{\eta}{\tau}\frac{h}{\phi} + \frac{4}{\pi}\frac{\eta^*}{\tau^*}\right) \quad (4)$$

Equations (2) and (4) are general equations accounting for drop-interface and drop-drop coalescence within the wedge under steady conditions, assuming that time and position average values of the volume packing efficiency in the wedge and area packing efficiency at the interface are acceptable. This implies that rearrangement of drops in the vicinity of a coalescence step, both at the interface and within the bed, is instantaneous, and that local disturbances in the vicinity of a coalescence step do not seriously affect the coalescence mechanism. These factors are currently being investigated in detail (*1*).

The success of this approach in analyzing performance data of dispersions depends on accurate data on coalescence times being available (*2* to *6*). Detailed studies have been carried out on drop-interface coalescence, and MacKay and Mason (*5*) Jeffreys and Hawksley (*6*) have proposed models to account for drop-interface coalescence. As a droplet approaches a plane interface, a film of the continuous phase is trapped between the deformed interface and the drop, and this film drains until at some critical thickness the film ruptures and the liquid in the drop drains into the bulk liquid. This mechanism is often interrupted and a secondary drop is formed which coalesces again in a similar manner. In some systems, up to eight stages have been observed (*7*). In practice, no one coalescence time is observed for a given system and drop size but rather a distribution of times is obtained. It has been shown that coalescence times for a given system can be represented by an equation of the form

$$\log_e N/N_0 = -K(t - t_0)^m \quad (5)$$

Values of m from 1.0 to 2.5 have been reported in the literature. Several attempts (*1, 2, 6, 10*) have been made to correlate mean rest times of a drop at an interface with physical parameters of the system. Thus, Jeffreys and Hawksley (*6*) proposed the equation

$$\tau^*_{1/2} = 4.53 \times 10^5 \left[\left(\frac{\mu_2^{0.5}\Delta\rho^{1.2}}{\gamma^2}\right)\left(\frac{T}{25}\right)^{-0.7\mu_2^{0.5}} \phi^{0.02} \left(\frac{\gamma^2}{\mu_2^{0.5}}\right)^{0.55} L^{0.001}\left(\frac{\gamma^2}{\mu_2^{0.5}}\right)\right]^{0.91} \quad (6)$$

while Smith (*1*) has correlated drop-interface coalescence times using the equation

$$\frac{\tau^*\gamma}{\mu\phi} \propto \left(\frac{\phi^2\Delta\rho g}{\gamma}\right)^{0.25} \quad (7)$$

and Lawson and Jeffreys (*9*) have proposed the equation

$$\frac{\tau^*\gamma}{\mu\phi} = 1.32 \times 10^5 \left(\frac{L}{\phi}\right)^{0.18}\left(\frac{\phi^2\Delta\rho g}{\gamma}\right)^{0.32} \quad (8)$$

Drop-to-drop coalescence has received very little attention because of the difficulties in studying this without interfering with the mechanism. MacKay and Mason (*11*), Kintner (*12*), and Van der Temple (*13*) have some data on coalescence of drops at curved surfaces and on the rupture of films. Smith (*7*) has developed a technique for studying drop-drop coalescence.

If the overall process is considered, the volume of dispersed phase entering the wedge per second must be equal to the volume of dispersed phase coalescing at the lower interface over the entire wedge. Interdroplet coalescence will affect this in so far as it will influence the average drop diameter, packing efficiencies, and mean coalescence times of the droplet at the lower interface. Thus, for small angles of inclination θ of the wedge

$$\sec.\ \theta \rightarrow 1.0 \quad (9)$$

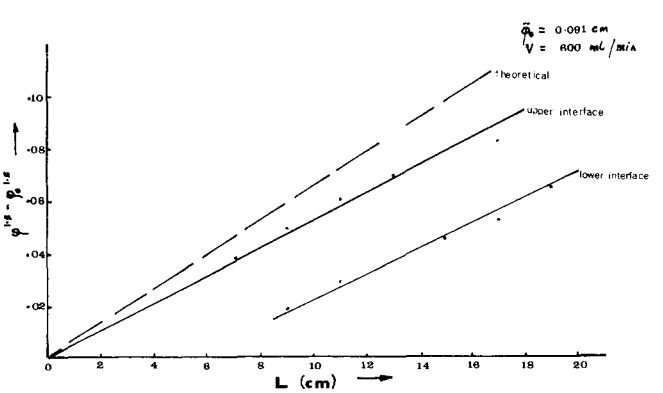

Fig. 4. Comparison of model, Equation (24), with experimental data. Kerosene dispersed.

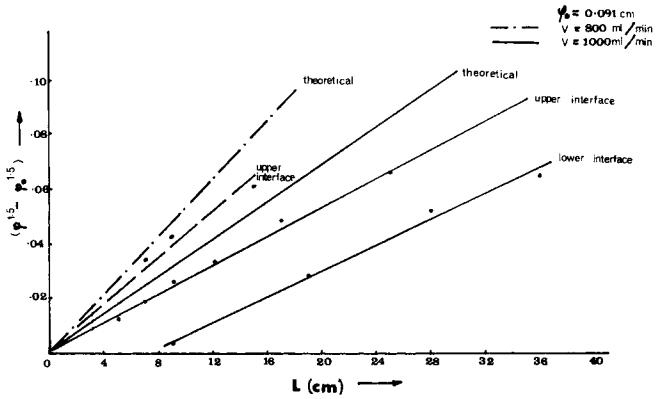

Fig. 5. Comparison of model, Equation (24), with experimental data. Kerosene dispersed.

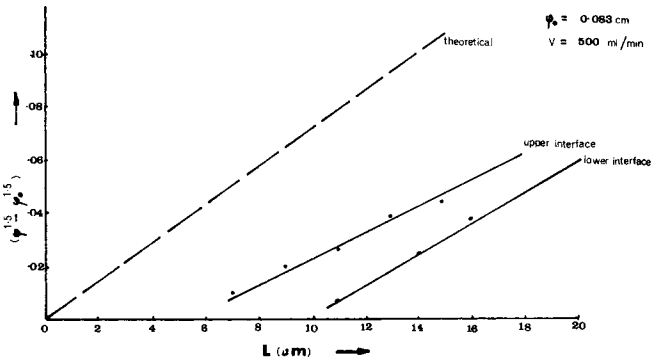

Fig. 6. Comparison of model, Equation (24), with experimental data. Kerosene dispersed.

and the length of the lower interface approximates to the wedge length L. Then

$$\frac{\pi n_0 \phi_0^3}{6} = \int_0^L \frac{\pi}{6} \frac{\phi^3 1}{\tau^*} \frac{\eta^*}{\frac{\pi\phi^2}{4}}\, dl \qquad (10)$$

where n_0 is the number of droplets of mean diameter ϕ_0 entering the wedge from the mixing stage per second.

Simplifying (10), we get

$$n_0 \phi_0^3 = \frac{4}{\pi} \int_0^L \frac{\eta^*}{\tau^*} \phi\, dl \qquad (11)$$

If the volumetric flow rate of dispersed phase to the settler is V_0, then

$$V_0 = H v_0 n_0 \qquad (12)$$

From (11), taking mean values, we get

$$V_0 = \frac{1}{3} \eta^* \int_0^L \frac{\phi}{\tau^*}\, dl \qquad (13)$$

The boundary conditions for solution of Equations (2), (4), (12), and (13) are

$$l = 0,\ n = n_0,\ \phi = \phi_0 \qquad (14)$$

$$\lim_{l \to L} \quad n = 0 \qquad (15)$$

$$\lim_{l \to L} \quad \phi = \phi_L \qquad (16)$$

or

$$\lim_{l \to L} \quad h = \phi_L \qquad (17)$$

Equations (16) and (17) express the condition that at the end of the wedge a single row of drops of mean diameter ϕ_L exist. Equations (2) and (4) can be combined to give

$$\frac{d\phi}{dl} = \frac{\eta h}{\pi \tau n \phi^2} \qquad (18)$$

This equation is the basic equation for the design or analysis of gravity settlers. However, the relative effects of drop-interface and drop-drop coalescence on the separation process occuring can be illustrated more conveniently by solving Equations (2) and (4) numerically from the data from Part I for varying values of τ and τ^*. The results of these calculations are presented in Figures 2 and 3. Figure 2 illustrates the effect of increasing drop-interface coalescence times on wedge length and wedge thickness, while Figure 3 illustrates the effects of increasing drop-drop coalescence times or wedge length and final drop size. It will be seen that both processes affect the separation appreciably, which is contrary to the suggestions made by Ryan, Daley, and Lawrie (*14*) that most of the coalescence occurs at the coalescence interface rather than within the dispersion.

Table 1. System Water:Kerosene

Run No.	Dispersed phase	Flow rate dispersed phase, ml./min.	Inlet main drop diameter, cm.	Mean drop velocity, cm./sec.	Overall wedge length, cm.	Entrance length, cm.	Calculated slope, Equation (23)	f[Equation (22)], sec. cm.$^{2/3}$	Ratio of slopes predicted by model, Equation (23)	Experimental ratio of slopes, Fig. 5, 1 to 5, 4
1	Kerosene	600	0.091	0.50	20	0	0.00675	37	—	—
2	Kerosene	800	0.091	0.80	24	0	0.00563	37	$\frac{m_1}{m_2} = 1.2$	1.18
3	Kerosene	1,000	0.091	0.80	34	0	0.00421	37	$\frac{m_1}{m_3} = 1.6$	1.56
4	Kerosene	500	0.088	0.40	21	6	0.00845	37	—	—
5	Kerosene	600	0.083	0.50	27	6	0.00675	37	$\frac{m_4}{m_5} = 1.25$	1.4
6	Kerosene	700	0.083	0.60	31	10	0.00563	37	$\frac{m_4}{m_6} = 1.5$	1.6
7	Water	500	0.054	0.36	22.5	7	0.00470	73.8	—	—
8	Water	700	0.054	0.60	28.0	12	0.00282	73.8	$\frac{m_7}{m_8} = 1.6$	1.7

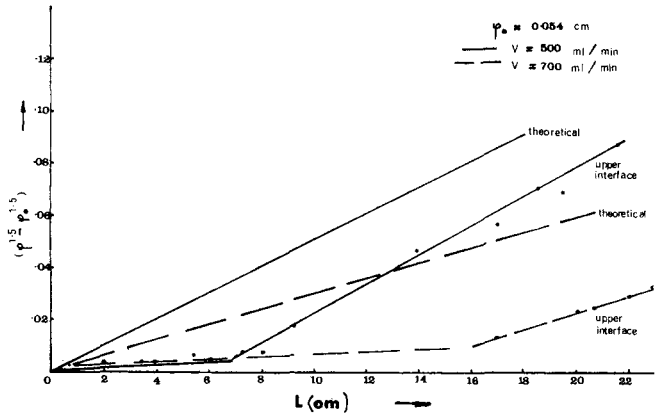

Fig. 7. Comparison of model, Equation (24), with experimental data. Water dispersed.

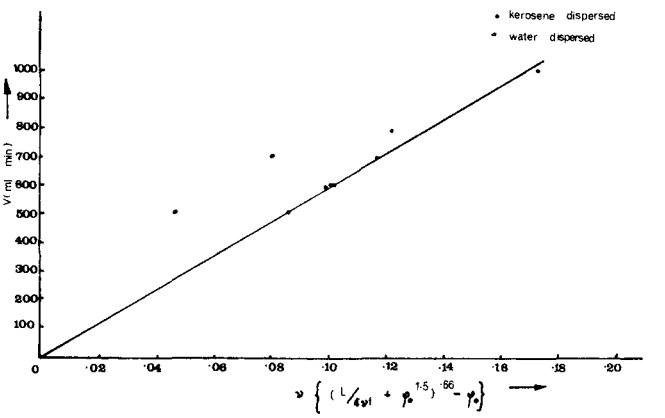

Fig. 9. Comparison of Equation (26) with experimental data.

At any position in the wedge

$$\nu h \eta = \frac{\pi}{6} n \phi^3 \tag{19}$$

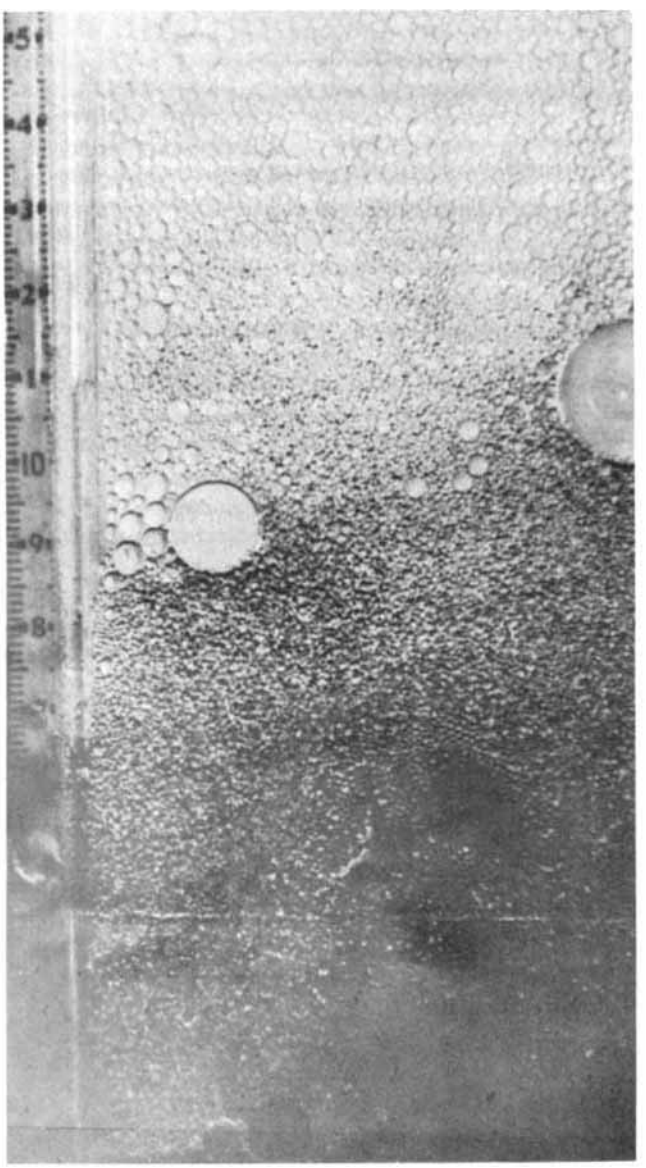

Fig. 8. Typical entry region for water dispersed. The photograph shows that the turbulence is not damped out in the first 7 cm. of the wedge. Coalescence is initiated after the drops have passed through this section.

Therefore, substituting Equation (19) into (18), we get

$$\frac{d\phi}{dl} = \frac{1}{6} \frac{\phi}{\nu\tau} \tag{20}$$

Previous experimental work (2 to 6) has shown that the coalescence time for drop-interface coalescence is a function of drop diameter, the coalescence time increasing with diameter. Very few results have been published correlating drop-drop coalescences time with size, but Smith's results (7) indicate that a similar relationship exists; that is, that

$$\tau = f \cdot \phi^{1.5} \tag{21}$$

where f is obtained from Equation (8). Then, assuming uniform velocity in the wedge, we get

$$\frac{d\phi}{dl} = \frac{1}{6\nu f \cdot \phi^{0.5}} \tag{22}$$

Integrating this equation between the limits (l, ϕ) and $(0, \phi_0)$ and rearranging, we obtain

$$\phi^{1.5} - \phi_0^{1.5} = \frac{l}{4\nu f} \tag{23}$$

In Table 1, experimental conditions and the calculated gradients of Equation (23) are tabulated; a comparison of this equation with the experimental results for the system kerosene—water are shown in Figures 4 to 7. From these figures it can be seen that the experimental results, when treated in this way, are adequately represented by a straight line. The lines shown are the result of regression analyses, the standard deviation being less than 0.6. The predicted results from Equation (23) are in every case somewhat higher; the ratio of the theoretical gradient from equation (23) to that obtained from the experimental results varies from 1.03 to 1.25. This can be explained, since the correlation of coalescence times of single drops was used in the analysis, and this cannot account for the interactions between droplets that affect the coalescence process (*10, 15*). Furthermore, it can be seen from the results that as the initial drop size decreases, corresponding to an increase in agitation in the mixer, and/or at higher volumetric flow rates in the settler, the conditions at the settler inlet change. Thus, the entrance region in which droplets rearrange to form a close packed structure increases, and the initial boundary condition, Equation (14), is not satisfied. This accounts for the displacement of the experimental results. The effect is illustrated in Figure 8 where, as the photograph shows, the disturbance can be seen in the center of the bed up to about 6 to 7 cm. from

the entry point. These disturbances could be due to back mixing effects brought about by sudden enlargement of the stream as it flows from the transfer line into the settler. This effect is more prominent as the inlet drop size decreases, as is confirmed by comparison of Figures 4 and 6. Furthermore, comparison of the results for kerosene drops coalescing with those for water drops coalescing, Figures 4 and 7, shows that for similar volume flow rates of dispersed phase, the mean inlet drop size for kerosene is much greater than the mean inlet drop size for water. When kerosene is the dispersed phase, coalescence commences almost immediately, whereas for water an entrance region in which the droplets were rearranging into a stable configuration was apparent up to 6 cm. from the inlet. This is confirmed in Figure 8, where significant coalescence does not take place until 6 cm. from the inlet. Hence, in the case of smaller droplets, the formation of a stable packing is delayed; the effect is more pronounced when kerosene is the dispersed phase because the viscosity of the continuous phase is lower.

If Equation (23) is applied to two experiments in which the initial mean drop diameter is the same, then, by assuming that interactions between adjacent drops are the same in each case, the theory predicts that the ratio of the slope of Equation (23) is inversely proportioned to the mean axial velocity of the drops in the settler. From Table 1 this prediction may be compared with the experimental results, and in all cases there is satisfactory agreement.

In the development of this model to account for the performance of gravity settlers, only axial flow of drops in the settler was considered. The experimental results obtained would indicate a different behavior at the upper and lower interface in the wedge, although both sets of data show the same trend when comparing experimental results with Equation (23). Subsequent experiments have shown small differences in the drop velocities at the upper and lower interfaces. For water drops settling from a water—kerosene emulsion, the mean velocity of droplets at the upper interface was slightly greater than the mean velocity of droplets at the lower interface. This indicates that there are small vertical displacements of drops within the emulsion. Smith and Davies (*1*) have shown that if a drop-to-drop coalescence takes place within a heterogeneous layer, the resulting larger drop can move relative to the density gradient to a new equilibrium position. This rearrangement takes place almost instantaneously. Furthermore, it appears from very recent work that the drop-to-drop coalescence rate varies throughout the wedge (over and above the influence of radii of curvature on coalescence times), being greater near the drop coalescing interface. This observation is being investigated and will form the basis of a subsequent paper.

Consider the overall flow rate of dispersed phase to the settler. Then, combining Equations (8), (13), and (23) and integrating between the limits $l = 0$ to $l = L$, we obtain

$$V_0 = 2\eta^* \nu \left[\left(\phi_0^{3/2} + \frac{L}{4\nu f} \right)^{2/3} - \phi_0 \right] \qquad (24)$$

A comparison of this equation with experimental data is shown in Figure 9, where a correction has been made to allow for the effect of the entrance region. It can be seen that satisfactory agreement between the model and experimental data is obtained.

CONCLUSION

For a given system, if the fundamental data on drop/interface and drop/drop coalescence times are known, then the model can be used to predict the mean drop size distribution throughout the wedge and the overall wedge length as a function of flow rates of the phases to the settler.

NOTATION

a = constant, Equation (5)
f = function in Equation (21), $TL^{-3/2}$
H = height of wedge at inlet, (L)
h = height of wedge, (L)
k = constant, Equation (5)
L = overall length of wedge, (L)
L' = distance of fall of drop, (L)
l = length of wedge, (L)
m = slope, Equation (5)
N = number of drops coalesced after t
N_0 = total number of drops
n = number of drops/second/width, $T^{-1}L^{-1}$
T = temperature, °C., θ
t = time, (T)
t_0 = initial drainage period, (T)
V_0 = volumetric flow rate/unit width of settler, (L^2T^{-1})

Greek Letters

ν = axial velocity of drops, (LT^{-1})
θ = angle subtended by wedge
η = volume packing efficiency of drops in wedge
η^* = area packing efficiency of drops at the interface
τ = mean drop-drop coalescence time, (T)
τ^* = mean drop-interface coalescence time, (T)
$\tau^*_{1/2}$ = half time coalescence times (t at $N/N_0 = 0.5$), (T)
ϕ = drop diameter or diameter of equivalent sphere, (L)
μ = viscosity, $(ML^{-1}T^{-1})$
γ = interfacial tension, (MT^{-2})
ρ = density

Subscripts

0 = conditions at inlet
2 = properties of continuous phase

LITERATURE CITED

1. Smith, D. V., and G. A. Davies, *I.S.E.C.*, The Hague (May, 1971).
2. Gillespie, T., and E. K. Rideal, *Trans. Faraday Soc.*, **52**, 173 (1956).
3. Elton, G. A. H., and R. G. Picknett, *Second intern. Congress Surface Activity*, **1**, 288 (1959).
4. Charles, G. E., and S. G. Mason, *J. Colloid Sci.*, **15**, 236 (1960).
5. MacKay, G. D. M., and S. G. Mason, *ibid.*, **16**, 632 (1961).
6. Jeffreys, G. V., and J. L. Hawksley, *AIChE J.*, **11**, 413 (1965).
7. Smith, D. V., M.Sc. thesis, Univ. Manchester, England (1965).
8. Hawksley, J. L., Ph.D. thesis, Univ. Birmingham, England (1963).
9. Lawson, G. B., and G. V. Jeffreys, *I.S.E.C.*, The Hague (May, 1971).
10. Chappelear, D. C., *J. Colloid Sci.*, **16**, 186 (1961).
11. MacKay, G. D. M., and S. G. Mason, *Can. J. Chem. Eng.*, **41**, 203 (1963).
12. McAvoy, R. M., and R. C. Kintner, *J. Colloid Sci.*, **20**, 18 (1965).
13. Van der Temple, M., *ibid.*, **13**, 125 (1958).
14. Ryan, A. D., F. L. Daley, and R. S. Lawrie, *U.S. Atom Energy Com. Report No. ORNL2591* (1960); *Chem. Eng. Progr.*, **55**, 70 (1959).
15. Smith, D. V., and G. A. Davies, *J. Interface Colloid Sci.*, to be published.

Manuscript received August 23, 1968; revision received February 7, 1969; paper accepted February 17, 1969. Paper presented at AIChE Salt Lake City meeting.